Effectiveness of gain control in EDFAs against traffic with different levels of bursty behaviour

M.Karásek, A.Bononi, L.A.Rusch and M.Menif

Abstract: Previous publications have addressed the impact of bursty, self-similar traffic on erbium-doped fibre amplifiers (EDFA). Several gain control techniques have been suggested to combat the gain fluctuations of EDFA with this type of traffic. The effectiveness of two such methods are investigated, namely highly inverted amplifiers and all-optical gain clamping, while varying the parameters characterising the burstiness of the sources. While previous publications have focused on the effect of the average load or activity factor, the paper further investigate the dependence on the relative variability of the packet burst lengths (ON times), and lengths of the interburst idle times (OFF times). Both gain control methods reduce the output power and signal-to-noise ratio excursions with respect to a standard amplifier chain. The authors find that, for an eight channel WDM system and a cascade of six EDFAs, all-optical gain clamping can reduce the variations by a factor of five, provided adequate power is present in the clamping laser, while highly inverted amplifiers have variations reduced by a factor of two. The authors find that, in a clamped chain, the source activity factor does not uniquely determine the required level of lasing power. The authors also deduce that information on the relative variability of ON and OFF times is essential.

1 Introduction

A serious problem facing wavelength division multiplexed (WDM) networks with fibre amplifier cascades is transient cross saturation or gain dynamics of fibre amplifiers. Attention has been focused primarily on circuit-switched scenarios. When the number of WDM channels transmitted through a circuit-switching network varies due to network reconfiguration or channel failure, channel addition/removal will tend to perturb signals at the surviving channels that share all or part of the route. Although this perturbation will generally be small in a single amplifier, it will grow rapidly along a cascade. Power transients in the surviving channels can cause severe service impairment due to either inadequate eye opening or the appearance of optical nonlinearities [1–4]. Several solutions to this problem have been proposed and experimentally verified. These include fast pump control [5, 6], fast link control by insertion of a control channel [7] and gain clamping by an all-optical feedback loop [8, 9].

Recent traffic measurements from working packet networks (including Ethernet local area networks, wide area networks, integrated services digital network, and variable bit rate video over asynchronous transfer mode) have shown features of self-similarity: i.e. realistic packet network traffic looks the same when measured over time scales ranging from seconds to minutes and hours [10–12]. It has been concluded that the superposition of many ON/OFF sources or packet trains with strictly alternating ON- and OFF- periods with infinite variance produces aggregate network traffic that is self-similar. When such packet traffic is directly transmitted in burst mode on the WDM channels, as in the case of Internet protocol (IP) over WDM, long interburst idle intervals may give enough time to fibre amplifiers to reach gains greatly exceeding the average values. This can, in turn, lead to significant variation in output power and optical signal-to-noise ratio (OSNR). This effect accumulates along a cascade of fibre amplifiers in the same way as the fast power transients in the circuit-switching scenario. The effect of WDM traffic statistics on the output power and optical OSNR swings in a cascade of five erbium-doped fibre amplifiers (EDFAs) of standard design, has been theoretically investigated in [13, 14]. The results of the simulations indicate that substantial power and OSNR swings occur at the output of a cascade when highly-variable burst-mode traffic is transmitted. Power swings in excess of 9 dBm and OSNR swings of more than 4 dB were observed. The stabilisation effect of clamping the gain of the first EDFA by all-optical feedback loop and letting the lasing power propagate through the cascade of three EDFAs has been demonstrated experimentally in [15].

This paper presents a theoretical analysis of output power and OSNR fluctuations in cascades of six EDFAs due to the variability of burst-mode packet-switched traffic transmitted through eight WDM channels. The effect of traffic burstiness and network utilisation factor on output power and OSNR swings has been investigated for three

IEE Proceedings online no. 20000567

DOI: 10.1049/ip-opt:20000567

Paper received 6th January 2000

M. Karásek, L.A. Rusch and M. Menif are with the Centre for Optics, Photonics and Lasers (COPL), Laval University, Department of Electrical and Computer Engineering, Québec, Canada G1K 7P4

A. Bononi is with the Università di Parma, Dipartimento di Ignegneria dell'Informazione I-43100 Parma, Italy

M. Karásek is on leave of absence from the Institute of Radio Engineering and Electronics, Academy of Sciences of the Czech Republic, Chaberska 57, 182 51 Prague

cascades: (*a*) cascade of six standard design, two-stage EDFAs, (*b*) cascade of two-stage, highly inverted EDFAs, and (*c*) all-optical gain clamped cascade in which only the first EDFA is clamped using a ring laser configuration and the lasing power propagates along the cascade. The analysis is based on the application of a dynamic spectrally resolved model of an EDFA. In this paper, the authors first solve the transcendental equation for the steady-state value of total number of excited erbium ions in the doped fibre of each amplifier. A transient analysis is then performed based on the assumption that the atomic populations remain constant during a time step δt of several hundreds of nanoseconds, so that direct time evolution of signal and ASE powers can be performed for time variable input WDM signals. The burst-mode packet-switched traffic is simulated by generating statistically independent ON and OFF intervals (packets) with a rounded Pareto distribution for each WDM channel. The effect of traffic burstiness has been investigated by varying the parameters of Pareto distribution for both the ON and OFF intervals.

2 Dynamic model of EDFA cascades

To study the effect of cross gain saturation in concatenated EDFAs on highly variable packetised traffic, the authors will investigate the time-dependent output power and OSNR fluctuations in a cascade of six EDFAs concatenated with five transmission fibres of span loss $L = 20$ dB. shown schematically in Fig. 1*a* and *b*. Time-varying signals simulating asynchronous eight channel traffic (channels placed between 1547 and 1554 nm with 1 nm spacing) were randomly generated in a way similar to that described in [14]. To demonstrate the differences between the standard, strongly inverted and gain clamped cascades, simulation of the highly variable input traffic was performed for three different cascades:

Case (*a*): cascade of six equal two-stage EDFAs of standard design and gain equalising filter as shown in the inset of Fig. 1*a* ($\ell_1 = 12$ m, $P_{p1} = 9$ mW, $\ell_2 = 13$ m, $P_{p2} = 40$ mW);

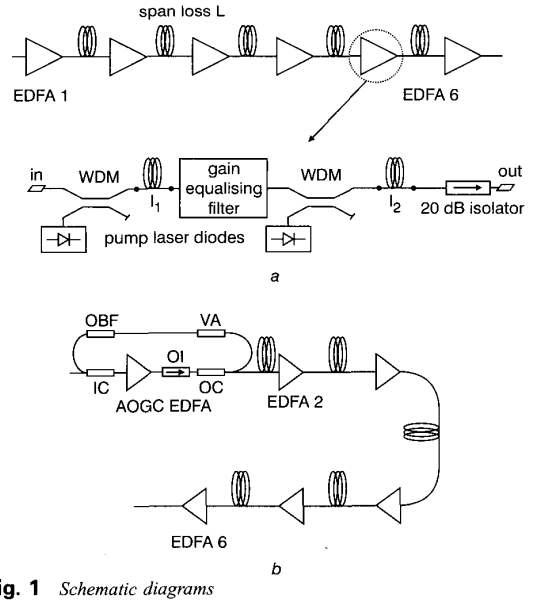

Fig. 1 *Schematic diagrams*

a Cascade of six two-stage EDFAs, the inset shows a single repeater. *b* Gain clamped cascade of six EDFAs: OBF = optical bandpass filter; OI = optical isolator, VA = variable attenuator; IC, OC = input and output couplers.

Case (*b*): cascade of six equal two-stage EDFAs with strongly inverted doped fibers and a gain equalizing filter ($\ell_1 = 10$ m, $P_{p1} = 70$ mW, $\ell_2 = 11.3$ m, $P_{p2} = 200$ mW);

Case (*c*): cascade of single-stage EDFAs with gain equalising filter. The first amplifier is gain clamped by ring laser configuration, Fig. 1*b* (gain clamped EDFA: $\ell = 30$ m, $P_p = 65$ mW, EDFAs numbers 2 to 6: $\ell = 25$ m, $P_p = 49$ mW).

The model used for the simulations is based on the dynamic model of EDFA derived in [16] under the assumption of homogeneously broadened gain medium and absence of excited-state absorption. In contrast to [16], the amplified spontaneous emission is taken into account in the model used in this paper, in accordance with [17]. The wavelength region from 1450 nm to 1650 nm is resolved in M bins of constant width $\Delta\lambda$. Let $\mathcal{A}$ denote the set of all ASE bins, and $\mathcal{S}$ denote the set of bins on which the WDM signals, the gain stabilising lasing power (in case of gain clamped cascade *c*) and the pump fall (the bin width is small enough such that, at most, one signal per bin is present, located at its centre). Dynamic behaviour of each doped fibre in the cascade is described by a single ordinary differential equation for time evolution of the total metastable level population, $r(t)$, referred to as the *reservoir*, $r(t) = \int_0^{2\pi}\int_0^{\infty}\int_0^{\ell} n_2(\rho, \phi, z, t)\rho\, dr d\phi\, dz$, where $n_2(\rho, \phi, z, t)$ is the population density of the $^4I_{13/2}$ metastable level, ℓ is the length of the erbium-doped fibre (EDF), and ρ, ϕ, z are the cylindrical co-ordinates. The equation describing the time evolution of the reservoir $r_k(t)$ at EDF number k is given by

$$\frac{\mathrm{d}}{\mathrm{d}t} r_k(t) = -\frac{r_k(t)}{\tau} + \sum_{i\in\{\mathcal{S},\mathcal{A}\}} Q_{i,k}^{\mathrm{in}}(1 - G_{i,k}(r_k(t))) - \sum_{i\in\mathcal{A}} 4n_{i,k}^{sp}(r_k(t))(G_{i,k}(r_k(t)) - 1)\Delta\nu_i \quad (1)$$

where τ is the spontaneous lifetime of the metastable level; $Q_{i,k}^{in}$ is the signal or pump (if $i \in \mathcal{S}$) or external ASE photon flux (if $i \in \mathcal{A}$) [ph/s] entering doped fibre k at wavelength λ_i corresponding to wavelength bin i ($Q_{i,k} = P_{i,k}/h\nu_i$, where $h\nu_i$ is the photon energy and ν_i is the frequency of bin i). Signal fluxes are distinguished from ASE fluxes even when occupying the same wavelength bin, in order to be able to evaluate the OSNR at the doped fiber output; $G_{i,k}(\tau_k(t)) = \exp(B_{i,k}r_k(t) - A_{i,k})$ is the gain at λ_i of EDFA k, where $A_{i,k}$, $B_{i,k}$ are nondimensional coefficients, dependent on frequency ν_i through the erbium ions absorption and emission cross-sections:

$$A_{i,k} \triangleq \alpha_i\ell_k,\ B_{i,k} \triangleq (g_i + \alpha_i)/(\rho A_{\mathrm{eff}})$$

ρ being the erbium concentration [m^{-3}], A_{eff} the effective area of the doped part of the fibre core [m^2], ℓ_k is the length of the kth doped fibre [m]; and $\alpha_i \triangleq \rho\Gamma_i\sigma_i^a$ and $g_i \triangleq \rho\Gamma_i\sigma_i^e$ are the absorption and emission constants; Γ_i is the confinement factor at λ_i calculated by the overlap integral between the radial distribution of the LP_{01} mode intensity and the erbium ions doping distribution; σ_i^a and σ_i^e[m^2] are the absorption and emission cross-sections at λ_i, respectively; $n_{i,k}^{sp}(r_k(t)) = g_i r_k(t)/((g_i + \alpha_i)r_k(t) - \alpha_i\rho A_{eff}\ell_k)$ is the spontaneous emission factor, and the summation in which it appears in eqn. 1 represents the ASE generated inside doped fibre k, the factor 4 representing two polarisation components for both forward and backward ASE; $\Delta\nu_i$ is the frequency width [Hz] of wavelength bin i.

When calculating the signal and ASE fluxes at the output of EDFA k in cascades (a) and (b), it is necessary

to differentiate between odd and even amplifiers. The authors assume that each repeater is a two-stage EDFA with a gain equalising filter that perfectly equalises the gain of the first stage over the signals wavelength range. The signal and ASE fluxes at the output of doped fibres $k=1, 3, \ldots, 11$ are given as follows:

$$Q^{\text{out}}_{i,k}(t) = Q^{\text{in}}_{i,k}(t)G_{i,k}(r_k(t))F_{i,k} \qquad i \in \mathcal{S}$$

$$Q^{\text{out}}_{i,k}(t) = \{Q^{\text{in}}_{i,k}(t)G_{i,k}(r_k(t)) + 2n^{sp}_{i,k}(t)(G_{i,k}(r_k(t)) - 1)\Delta\nu_i\}F_{i,k} \qquad i \in \mathcal{A} \quad (2)$$

where $F_{i,k}$ is the power transmission of the gain equalising filter k at wavelength λ_i. For the output fluxes at even doped fibres:

$$Q^{\text{out}}_{i,k}(t) = Q^{\text{out}}_{i,k-1}(t)G_{i,k}(r_k(t)) \quad k = 2, 4, \ldots, 12 \quad i \in \mathcal{S}$$

$$Q^{\text{out}}_{i,k}(t) = \{Q^{\text{out}}_{i,k-1}(t)G_{i,k}(r_k(t)) + 2n^{sp}_{i,k}(t)(G_{i,k}(r_k(t)) - 1)\Delta\nu_i\} \quad k = 2, 4, \ldots, 12 \quad i \in \mathcal{A} \quad (3)$$

In the above equations note that only half of the ASE generated in the EDFA, corresponding to forward ASE, is present at the output of the EDFA and will be propagated downstream. Also, the authors implicitly assume an isolator is placed between the two doped sections in each two-stage EDFA. Finally, indicating with L the loss of the transmission span between EDFAs (i.e. between even and odd doped fibres), the updated fluxes at the input of each odd doped fibre are as follows:

$$Q^{\text{in}}_{i,k}(t) = Q^{\text{out}}_{i,k-1}L \qquad k = 3, 5, \ldots, 11 \qquad i \in \{\mathcal{S}, \mathcal{A}\} \quad (4)$$

For the gain clamped cascade (c) with six EDFAs, Fig. 1b, the gain equalising filter is a part of each amplifier, so that eqn. 2 holds for $k=1, \ldots, 6$. Moreover, eqn. 4 holds for EDFAs $k=3, \ldots, 6$, while, for EDFA 2,

$$Q^{\text{in}}_{i,2}(t) = Q^{\text{out}}_{i,1}C^{\text{out}}L \qquad i \in \{\mathcal{S}, \mathcal{A}\} \quad (5)$$

Here C^{out} represents the coupling ratio of the output coupler (OC). The equations describing the optical feedback and characterising the input flux of the all optical gain clamped (AOGC) EDFA at each wavelength bin $i \in \{\mathcal{S}, \mathcal{A}\}$ are given as

$$Q^{\text{in}}_{i,1}(t) = Q^{\text{in}}_{\text{ext},i}(t)C^{\text{in}} + Q^{\text{out}}_{i,1}(t)(1 - C^{\text{out}})T_i\beta_{\text{va}}(1 - C^{\text{in}}) \qquad i \in \{\mathcal{S}, \mathcal{A}\} \quad (6)$$

In these equations, $Q^{in}_{ext,i}(t)$ is an external photon flux representing a WDM signal entering the cascade of EDFAs at wavelength λ_i, which is zero for $i \in \{\mathcal{A}\}$; C^{in} is the coupling ratio of the input coupler (IC), T_i is the power transmission of the optical bandpass filter (OBF) at wavelength λ_i, and β_{va} is the attenuation of the variable attenuator (VA). The optical bandpass filter effectively suppresses most of the ASE components fed back from the output to the input of the AOGC EDFA, so that a lasing action occurs with $Q^{in}_{las}(\lambda_{las})$ being the lasing photon flux at the input of EDF number 1. For the solution of the reservoir equations at EDFAs $2, \ldots, 6$ the laser flux is treated as an external signal flux in eqn. 1.

Numerical solution to the time-dependent eqn. 1 is separated into two steps: first, the steady-state value of r_k for each doped fibre in the cascade is determined for continuous-wave (CW) input signals, followed by a time evolution of $r_k(t)$ with burst-mode WDM traffic at the input to doped fibre number 1, $Q^{in}_{i,1}(t)$. To obtain a steady-state value of r_k, a transcendental equation derived from eqn. 1 by setting $dr_k(t)/dt = 0$ is solved numerically for $k=1, 2, \ldots$, starting with doped fibre number 1. In the case of the gain clamped cascade (c), the transcendental equation for EDFA 1 is more complicated due to the optical feedback loop implemented in this amplifier. In addition to the state variable r_1, the laser flux Q^{in}_{las} has to be found. An iterative solution was used to solve the transcendental equation for the steady-state value of r_1, while the transcendental equations for steady-state r_k, $k=2, \ldots, 6$ are solved directly. For the dynamic analysis, the power of each WDM channel is modulated according to an ON/OFF slotted renewal process. Using random numbers U_i, $(i=1, 2, \ldots 8)$, with uniform distribution on [0, 1], statistically independent ON and OFF bursts (composed of random integer number of slots) were generated for each WDM channel with a rounded Pareto distribution

$$T_{i,\text{ON}} = \left\lfloor \frac{1}{U_i^{(1/\gamma_{\text{ON}})}} \right\rfloor, \qquad T_{i,\text{OFF}} = \left\lfloor \frac{1}{U_i^{(1/\gamma_{\text{OFF}})}} \right\rfloor \quad (7)$$

where γ_{OFF} and γ_{ON} are parameters indicating the burstiness of the traffic (assumed to be the same for all WDM channels) and $\lfloor x \rfloor$ is the floor function.

3 Numerical results

In this analysis, the authors consider a typical Lucent Technologies EDF pumped at 1480 nm. The ASE power spectrum is taken into account over the region from 1450 to 1650 nm, subdivided into $M=200$ bins of equal width $\delta\lambda = 1$ nm. The gain equalisation filter with an insertion loss of 0.5 dB has been considered [18]. The coupling ratios of the input and the output couplers of cascade (c) were assumed to be $C^{in}=0.9$ and $C^{out}=0.5$, respectively. The time slot duration was set to 2.82μs (corresponding to 53 bytes at a bit rate of 150 Mbyte/s). The packets filling the ON slots were sampled at 10 points per slot, so that the time step for the solution of eqn. 2 was $\delta t = 0.282\mu s$. Simulation of the highly variable input traffic was performed over more than ten million time steps, corresponding to 3 s of transmission time. It was assumed that '1' and '0' bits within each packet are equally likely. The average utilisation of the aggregate WDM traffic is given by the utilisation factor u:

$$u = \frac{\sum_{i=1}^{8} E[T_{i,\text{ON}}]}{\sum_{i=1}^{8} E[T_{i,\text{ON}}] + \sum_{i=1}^{8} E[T_{i,\text{OFF}}]} \quad (8)$$

where $E[T_{i,\text{ON}}]$, $E[T_{i,\text{OFF}}]$ are the mean values of the ON and OFF bursts (in slot units) of individual WDM channels. All three cascades have been optimised for an aggregate utilisation of 50%. The lengths and pump powers of individual doped fibre sections have been selected to obtain EDFA gain of 20 dB, for CW power at the input of the first amplifier, $P^{in}_{i,1} = -20$ dBm/channel, in case of cascades (a) and (b), and -23 dBm/channel, in case of cascade (c), to compensate for the span loss $L=20$ dB and keep the signal level constant along the cascade. The first EDFA of the gain clamped cascade (c) has been designed to have gain of 23 dB to compensate for the additional 3 dB loss of the output coupler. The lasing wavelength was set at $\lambda_{las}=1558$ nm, the EDF length $\ell=30$ m and pump power power $P_p=65$ mW of the gain clamped EDFA give the intracavity lasing power $P^{intra}_{las}=20$ mW. As $C^{out}=0.5$, one half of this power propagates along the cascade (c) together with the highly variable WDM traffic and stabilises the gain of subsequent amplifiers.

3.1 Characteristics of the input traffic

The rounded Pareto distribution used by the authors to generate the highly variable input traffic is a *heavy - tailed* hyperbolic distribution, very similar to the Zipf (or Zeta) distribution [19]. Many properties of heavy-tailed distributions are qualitatively different from more commonly encountered distributions. If $1 < \gamma < 2$, then the Pareto distribution has infinite variance, and if $\gamma \leq 1$ then even the mean is infinite. As per eqn. 7, the authors have used the rounded Pareto distribution to generate ON and OFF bursts of the WDM traffic. Fig. 2 compares the theoretical values of the mean and variance of the ON burst length as a function of γ against the values attained in the authors realisation of the rounded Pareto distribution. The mean and variance are reported in units of slots. The discrete points correspond to simulation results, while the continuous curves correspond to theoretical values for the mean and variance of a rounded Pareto distribution, i.e. $mean = \sum_{k=1}^{N} 1/(k^{\gamma})$ and $variance = \sum_{k=1}^{N} (2k-1)/(k^{\gamma})$, where the summations have been arrested to N terms, where $N \cong 10^7$ is the total number of simulated time slots. Note that the summation for the variance would diverge to infinity for $N \rightarrow \infty$. It is noted that the mean of the randomly generated bursts matches the theory well, while the variance of the simulated bursts is lower than in theory, meaning that the simulation has a slightly more benign traffic than planned.

The self-similarity of the aggregate traffic at the input to the first EDFA with independently generated ON and OFF intervals was tested using the aggregate variance method (AVM) [20]. The time series $\mathbf{X} = \{X_i,\ i = 1,\ 2, \ldots, N\}$ representing 3 s of traffic generated by summing the instantaneous input signal powers over all eight WDM channels, at each sampling point, was divided into blocks of size m. The average power within each block was determined and a new time series $\mathbf{X}^{(m)} = \{X_k^m = 1/m \sum_{(k-1)m+1}^{km} X_i,\ k = 1,\ 2, \ldots, N/m\}$ generated. The variance of $\mathbf{X}^{(m)}$ was plotted against m in a log-log scale. A straight line with negative slope β greater than -1 is indicative of self-similarity, and the *Hurst* parameter, H, is given by $H = 1 + \beta/2$. For self-similar traffic with long-range dependence, $1/2 < H < 1$. As $H \rightarrow 1$, the degree of both self-similarity and long-range dependence increases. Results of the AVM analysis of 3 s of aggregate input traffic are shown in Fig. 3*a*, for three different degrees of burstiness. The slopes of the log(variance) against log(m) were estimated using least-squares regression as $\beta = -0.128$, -0.208 and -0.44, yielding estimates for $H = 0.994$, 0.896 and 0.779, for $\gamma_{ON} = \gamma_{OFF} = 1.10$, 1.30, and 1.80, respectively. Part of the aggregate input traffic (time series $\mathbf{X}$) for 5 ms $< t <$ 6 ms is shown in Fig. 3*b*.

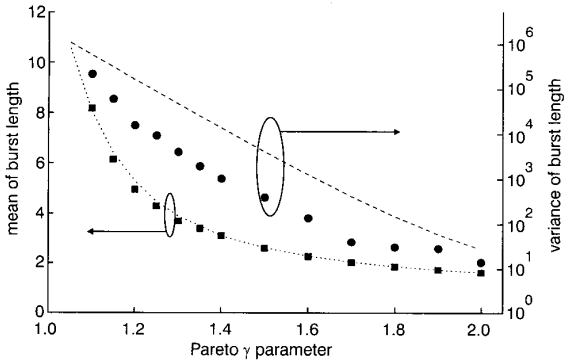

Fig. 2 *Dependence of mean and variance of packet length on Pareto distribution parameter* γ

Discrete points calculated from 10^7 randomly generated packets, lines obtained from mean $= \sum_{k=1}^{N} 1/(k^{\gamma})$, variance $= \sum_{k=1}^{N} (2k-1)/(k^{\gamma})$, $N = 10^7$.

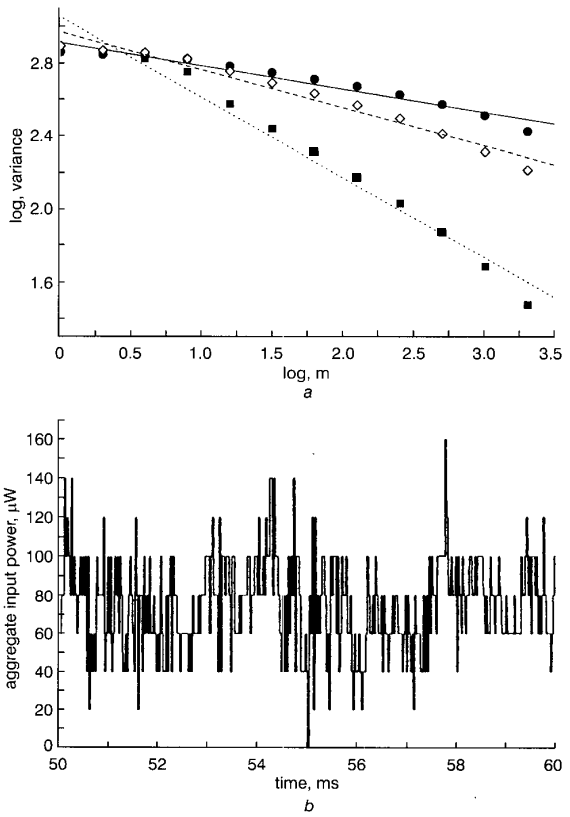

Fig. 3 *Results of AVM analysis of 3s of aggregate input traffic*

a AVM plot for 3 seconds of aggregate eight channel WDM traffic;
b Time evolution of 1 ms of traffic
● $\gamma_{ON} = \gamma_{OFF} = 1.10$, $H = 0.994$; ◇ $\gamma_{ON} = \gamma_{OFF} = 1.30$, $H = 0.896$; ■ $\gamma_{ON} = \gamma_{OFF} = 1.80$, $H = 0.779$

The probability that exactly i channels are simultaneously ON can be easily found to be:

$$P\{i \text{ ONs}\} = \binom{8}{i} u^i (1-u)^{(8-i)}$$

so that, for instance, for $u = 30\%$ the probability of all eight channels being OFF at the same time is about 5%. Owing to the random nature of the input traffic in individual WDM channels, output power and OSNR fluctuations caused by gain cross saturation were evaluated statistically. Histograms of output power and OSNR were calculated at each EDFA along the cascade for all eight WDM channels and probability mass function (PMF) has been plotted as a function of output power or OSNR. The OSNR is evaluated over an optical bandwidth of 1 nm. The effect of traffic variability and network utilisation on output power and OSNR fluctuations has been investigated by varying γ_{ON}, γ_{OFF} parameters of the input traffic. The spread of output power and OSNR probability mass function at a level of 10^{-2} has been selected as a criterion to quantify the spread resulting from packetised bursty WDM traffic.

3.2 Cascade of two-stage EDFAs of standard design: case (a)

The authors begin in Fig. 4 with the evolution of steady-state output power along cascade (*a*), when all eight WDM

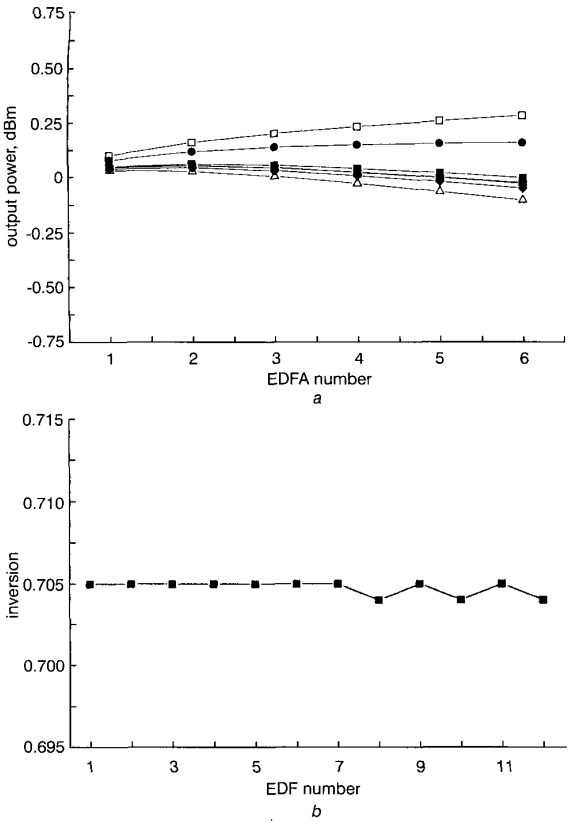

Fig. 4 *Evolution of steady state output power along cascade (a)*

a CW input power P_{1i}^{in}, = −20 dBm/channel;
–□– 1545 nm
–●– 1546 nm
–△– 1547 nm
–▼– 1548 nm
–○– 1549 nm
–■– 1550 nm
b evolution of steady-state *reservoir* at individual EDFAs
–△– 1551 nm
–◆– 1552 nm

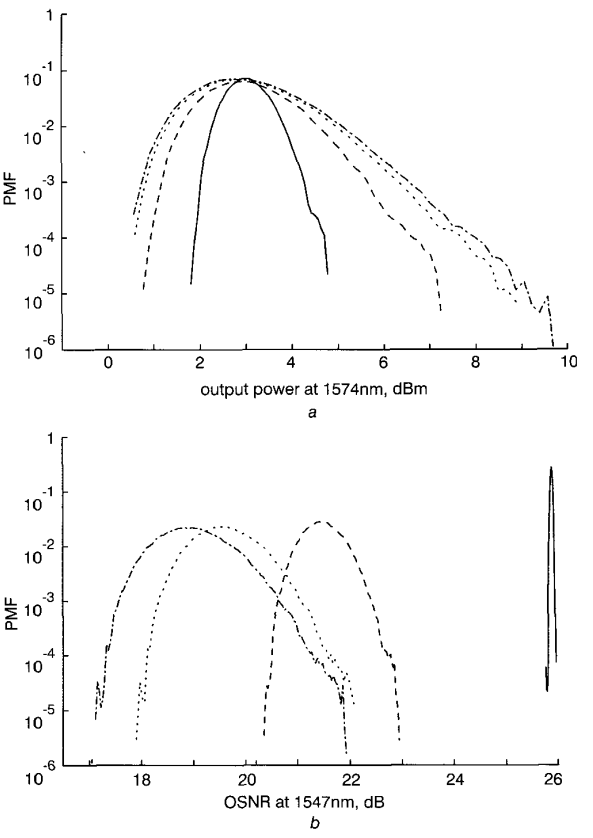

Fig. 5 *Plots of output power and OSNR*

a Probability mass function of signal power at $\lambda = 1547$ nm at the output of repeater 1, 3, 5 and 6: cascade (a), $\gamma_{ON} = \gamma_{OFF} = 1.20$, $u = 50\%$;
b Probability mass function of OSNR at $\lambda = 1547$ nm at the output of repeater 1, 3, 5 and 6: cascade (*a*), $\gamma_{ON} = \gamma_{OFF} = 1.20, u = 50\%$
–·–· EDFA 6
····· EDFA 5
– – – EDFA 3
—— EDFA 1

channels are transmitted with CW power at the input of the first EDFA $P_{i,1}^{in} = -20$ dBm/channel. It is seen that the gain of each EDFA compensates the loss of the transmission fibre. Owing to gain equalising filters the interchannel power spread between the weakest channel at 1551 nm and the strongest one at 1545 nm is only 0.39 dB. Fig. 4*b* shows the corresponding values of a steady-state normalised reservoir (i.e. the average inversion) of individual EDFAs. The average inversion is almost constant for both doped fibres of each EDFA and equal to 0.705. The plots of output power and OSNR evaluated at the output of EDFAs 1, 3, 5 and 6 for the channel at wavelength of 1547 nm are given in Figs. 5*a* and 5*b* respectively, for input traffic with utilisation of 50 % and $\gamma_{ON} = \gamma_{OFF} = 1.20$. The plots are obtained by tiling the power/OSNR range of interest with bins of equal size, and by cumulating the number of occurrences in each bin. Finally, the count in each bin is divided by the total bin count, so that an estimated probability mass function (PMF) is obtained. It is seen that the mean value of output power does not change along cascade (*a*), the mean OSNR decreases from 22.5 dB at EDFA 1 to 18.5 dB at EDFA 6. For both the output power and the OSNR, the fluctuations grow along the cascade, with spreads having probabilities larger than 10^{-2} of 1.52, 3.03, 3.68 and 3.93 dB, for output power after repeater 1, 3, 5 and 6, respectively. Spreads in OSNR after repeater 1, 3, 5 and 6 were 0.88, 1.0, 1.43 and 1.54 dB, respectively. To illustrate the dynamic behaviour of individual WDM channels, Figs. 6*a* and 6*b* show the PDF of output power and OSNR at the output of EDFA 6 for channels at 1545, 1547, 1549 and 1551 nm. The dynamic interchannel power spread corresponds to the CW spread plotted in Fig. 4. Spreads in OSNR probability mass function of individual WDM channels at the level of 10^{-2} are almost identical.

The effect of the utilisation factor and the burstiness of the aggregate WDM traffic are demonstrated in Fig. 7. In Fig. 7*a* the output power excursions averaged over all 8 WDM channels are plotted against the Pareto γ values of both the ON and the OFF bursts, for a fixed activity factor u. In the Figure, three values for the activity factor have been considered: $u = 30\%$ (circles), $u = 50\%$ (squares) and $u = 70\%$ (triangles). Consider, for instance, the curves joining triangles. The curve with upward triangles refers to the γ of ON bursts, γ_{ON}, varying from 1.04 to 1.3. For each upward triangle there is an associated downward triangle that indicates the value of the γ of OFF bursts, that gives $u = 70\%$, as per eqn. 8. The associated γ_{OFF} values vary from 1.2–1.99.

Several conclusions can be drawn from these graphs. Clearly, the excursions vary with the activity factor. Larger excursions occur with lower activity factor. This is due to longer times with no power being transmitted on a channel,

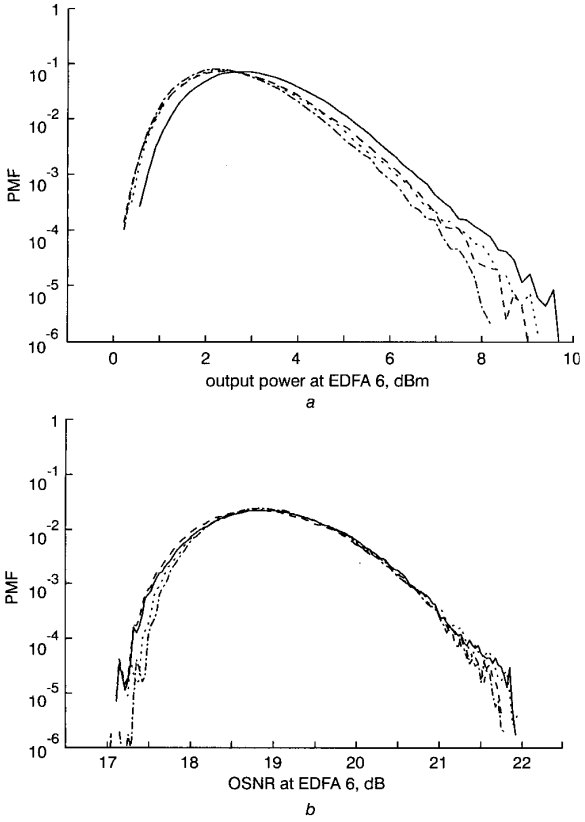

Fig. 6 *Illustration of the dynamic behaviour of individual WDM channels*

a Probability mass function of signal power at the output of repeater 6 for channels at $\lambda = 1547$, 1549, 1551 and 1553 nm: cascade (a), $\gamma_{ON} = \gamma_{OFF} = 1.20$, $u = 50\%$;
b Probability mass function of OSNR at the output of repeater 6 for channels at $\lambda = 1547$, 1549, 1551 and 1553 nm: cascade (a), $\gamma_{ON} = \gamma_{OFF} = 1.20$, $u = 50\%$
—— 1547 nm
– – – 1549 nm
····· 1551 nm
–·–· 1553 nm

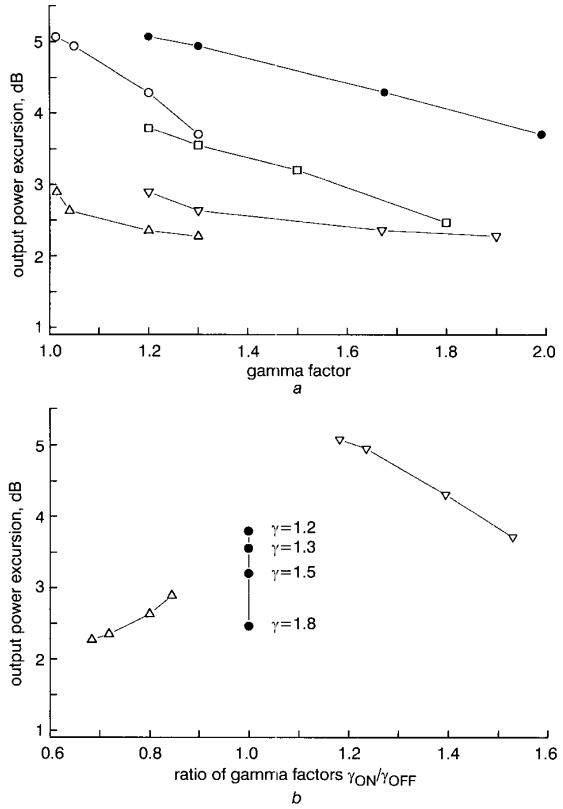

Fig. 7 *Plots to illustrate effect of utilisation factor and the burstiness of aggregate WDM traffic*

a Output power fluctuations with probability greater than 10^{-2} as a function of γ parameter, case (*a*);
–●– γ_{ON}, $u = 30\%$
–○– γ_{OFF}, $u = 30\%$
–□– γ_{OFF}, γ_{ON}, $u = 50\%$
–△– γ_{ON}, $u = 70\%$
–▽– γ_{OFF}, $u = 70\%$
b Output power fluctuations with probability greater than 10^{-2} as a function of ratio γ_{ON}/γ_{OFF}, case (*a*)
–△– $u = 70\%$
–●– $u = 50\%$
–▽– $u = 30\%$

and, therefore, more time for the reservoir to charge and provide higher gains. Larger activity factors lead to channels being more densely 'ON' and therefore leave the reservoir drained to the nominal steady-state value. However, there is clearly a second dependence on the relative values of the gamma parameters. The smaller the gamma parameter, the more bursty the traffic and the greater variability of ON and OFF times relative to their average values. When gamma exceeds two, the traffic is no longer characterised by infinite variance. In Fig. 7*a* with activity factor 30 % and γ_{OFF} varying (symbol ○), it can be seen that, for fixed activity factor, the excursion varies steeply with the gamma factor, whereas it varies less dramatically with activity factor 70 %.

In order to sort out the dependence on γ_{ON} against γ_{OFF}, and, in order to take into account eqns. 7 and 8, Fig. 7*b* shows plots of the output power swings at the output of cascade (*a*) against the ratio γ_{ON}/γ_{OFF}. To the right, there are larger values of γ_{ON} (larger variability in the OFF times) and to the left larger values of γ_{OFF} (larger variability in the ON times). The curve for activity factor 50 % is a vertical line at ratio one. As the gamma factor grows from 1.2 (high variability) to 1.8 (moderate variability), the excursions fall as the authors would expect. The importance of considering not only the activity factor but also the level of variability of the traffic, in order to assess the magnitude of the variability, can now be appreciated.

3.3 Cascade of two-stage EDFAs of strongly inverted design: case (b)

The parameters of the cascade of strongly inverted EDFAs, case (*b*), have been selected to obtain steady-state population inversion in individual doped fibres equal to $r_k = 0.755$, $k = 1, 2, \ldots, 12$. This inversion is close to the limiting value $r_{lim} = \sigma_e(\lambda_p)/(\sigma_e(\lambda_p) + \sigma_a(\lambda_p))$, which, for $\lambda_p = 1480$ nm, is $r_{lim}(1480) = 0.766$. Owing to higher inversion in the doped fibres, the cascade is less sensitive to bursty traffic than cascade (*a*), as is apparent from Figs. 8*a* and 8*b*, where the output power excursions with probability higher than 10^{-2} averaged for all eight channels at the output of cascade (*b*) are shown in the same way as in Figs. 7*a* and 7*b* for cascade (*a*). In comparison with cascade (*a*), fluctuations of output power and OSNR at the end of the cascade (*b*) are reduced by $\approx 50\%$. The dependence of these fluctuations on traffic parameters follows the same rules as in the case of cascade (*a*): (*i*) the higher the utilisation factor, the narrower is the spread

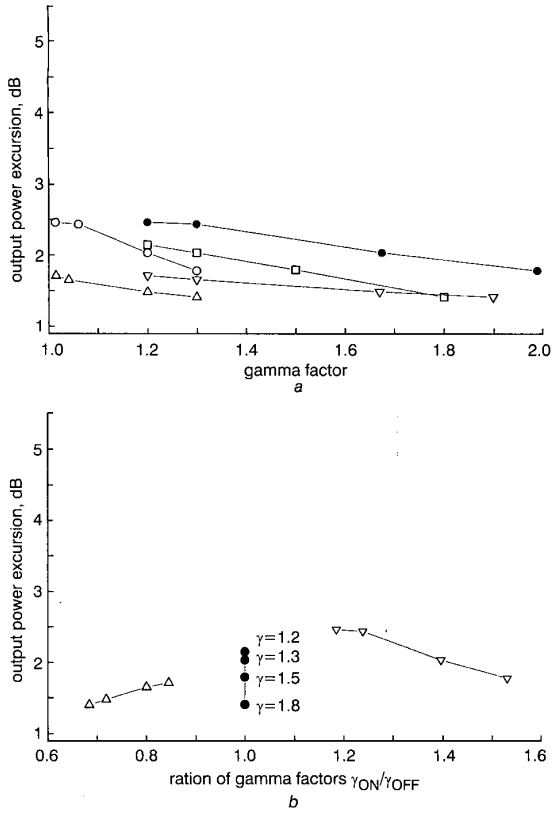

Fig. 8 *Output power fluctuations with probability greater than* 10^{-2}
a As a function of γ parameter, case (b);
-○- γ_{OFF}, $u=30\%$
-●- γ_{ON}, $u=30\%$
-□- γ_{OFF}, γ_{ON}, $u=50\%$
-△- γ_{ON}, $u=70\%$
-▽- γ_{OFF}, $u=70\%$
b As a function of ratio γ_{ON}/γ_{OFF}, case (*b*)
-△- $u=70\%$
-●- $u=50\%$
-▽- $u=30\%$

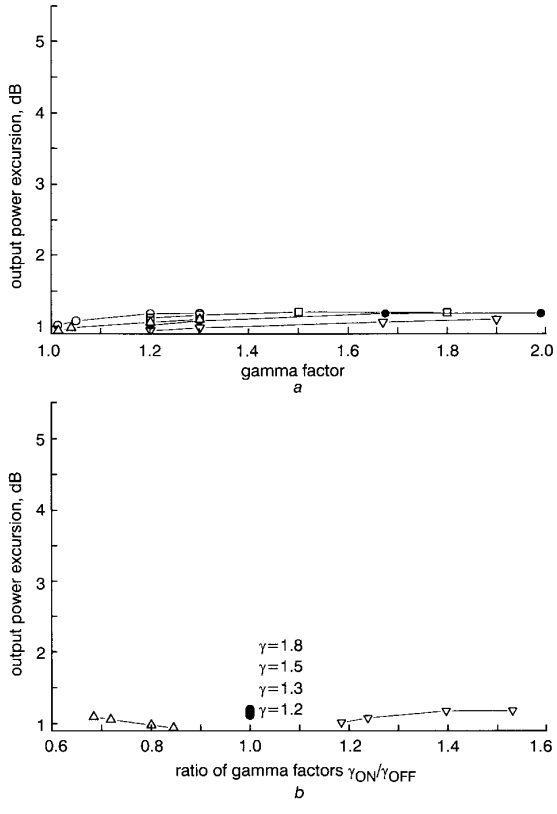

Fig. 9 *Output power fluctuations with probability greater than* 10^{-2}
a As a function of γ parameter, case (*c*);
-○- γ_{OFF}, $u=30\%$
-●- γ_{ON}, $u=30\%$
-□- γ_{OFF}, γ_{ON}, $u=50\%$
-▽- γ_{OFF}, $u=70\%$
-△- γ_{ON}, $u=70\%$
b As a function of ratio γ_{ON}/γ_{OFF}, case (*c*)
-△- $u=70\%$
-●- $u=50\%$
-▽- $u=30\%$

in PDF, (*ii*) smaller spread in output power and OSNR can be expected for traffic with the same u but greater γ_{OFF}.

3.4 Gain clamped cascade of single-stage EDFAs: case (c)

The first amplifier of this cascade is gain clamped using ring laser configuration. Under steady-state conditions (eight WDM channels with CW input power of $P_{1,i}^{in}=-23$ dBm/channel), lasing power of $P_{las}^{out}=10$ dBm propagates along the cascade. Population inversion in individual amplifiers under steady-state conditions is equal to $r_1=0.69$, $r_k=0.703$, $k=2, 3, \ldots, 6$, almost the same as in case (*a*). Signal power fluctuations of individual channels caused by gain cross saturation and bursty WDM traffic in the other channels are substantially reduced due to the stabilisation effect of the lasing power, which effectively 'absorbs' the variability on the input signals. Variable burstiness of the aggregate traffic has been analysed for the same set of γ_{ON}, γ_{OFF} and u parameters as for cascades (*a*) and (*b*). Corresponding output power fluctuations with probability greater than 10^{-2}, averaged over all eight WDM channels, are summarised in Figs. 9*a* and 9*b*. Both the output power and OSNR fluctuations are five times smaller in comparison with cascade (*a*) and are almost independent of the utilisation factor and of the γ parameters.

4 Conclusion

A numerical model of a cascade of erbium-doped fibre amplifiers, based on the solution of one ordinary differential equation for time-dependent gain of each doped fibre section, has been used to simulate the effect of gain cross saturation on packet-switched burst-mode traffic in a WDM link. The authors have investigated the effect of traffic variability on output power and optical signal-to-noise ratio swings in three different cascades of EDFAs: (*a*) cascade of six equal two-stage EDFAs, with standard design; (*b*) cascade of six equal two-stage EDFAs with strongly inverted doped fibres; and (*c*) gain clamped cascade of six single-stage EDFAs with the first amplifier gain-clamped in a ring configuration. An eight channel WDM system has been considered, the input traffic on each channel being modelled as a succession of bursts of packet transmission (ON periods) alternated with bursts of inactivity (OFF periods). The packets had a fixed duration of 2.82 μs, corresponding to 53 bytes at a bit rate of 150 Mbyte/s. The ON bursts and OFF bursts (expressed in packet units) were modelled as independent random variables, each having a heavy-tailed rounded Pareto

distribution, and the aggregate traffic exhibited a self-similar behaviour. To capture the heavy tails of the output power and OSNR swings, the authors simulated about 10 million time slots, representing 3 seconds of traffic.

Output power and OSNR fluctuations caused by gain cross saturation were evaluated statistically. Normalised distributions (PMF) of output power and OSNR were calculated at the output of each EDFA along the cascade for all eight WDM channels, and plotted as a function of output power or OSNR. The effect of traffic burstiness has been investigated by varying the parameters of the rounded Pareto distribution for both the ON and OFF bursts. The simulation results demonstrate that swings in both the output power and noise figure can be reduced by 50 % when high population inversion is maintained in all amplifiers of the cascade. For cascades (*a*) and (*b*), the dependence of output power and OSNR fluctuations on traffic parameters follows the same rules: (*i*) the higher the utilisation factor, the narrower the spread in PMF; (*ii*) smaller spread in output power and OSNR can be expected for traffic with the same u but greater γ_{OFF}.

In comparison with an unclamped cascade of six conventional EDFAs, the variation in output power and OSNR at the probability level of 10^{-2}, at the end of a gain-clamped cascade (*c*), is reduced by a factor of five if the lasing power is only 1 dB above the aggregate signal power. In contrast to cascades (*a*) and (*b*), output power and OSNR fluctuations are almost independent of network utilisation factor and of γ parameters determining the burstiness of the aggregate traffic.

5 References

1 SUN, Y., SRIVASTAVA, A.K., ZYSKIND, J.L., SULHOFF, J.W., WOLF, C., and TKACH, R.W.: 'Fast power transients in WDM optical networks with cascaded EDFAs', *Electron. Lett.*, 1997, **33**, pp. 313–314

2 ZYSKIND, J.L., SUN, Y., SRIVASTAVA, A.K., SULHOFF, J.W., LUCERO, A.J., WOLF, C., and TKACH, R.W.: 'Fast power transients in optically amplified multiwavelength optical networks'. Proc. OFC'96 Technical Digest, San Jose, CA, Paper TD 31–1

3 KARASEK, M.: 'Fast power transients in concatenated Pr^{3+}-doped fluoride fiber amplifiers', *J. Lightwave Technol.*, 1998, **16**, pp. 358–363

4 HAYEE, M.I., and WILLNER, A.E.: 'Transmission penalties due to EDFA gain transients in add/drop multiplexed WDM networks', *IEEE Photonics Technol. Lett.*, 1999, **11**, pp. 889–891

5 SRIVASTAVA, A.K., SUN, Y., ZYSKIND, J.L., and SULHOFF, J.W.: 'EDFA transient response to channel loss in WDM transmission system', *IEEE Photonics Technol. Lett.*, 1997, **9**, pp. 386–388

6 KARASEK, M., and VAN DER PLAATS, J.C.: 'Analysis of dynamic pump-loss controlled gain-locking system for erbium-doped fiber amplifiers', *IEEE Photonics Technol. Lett.*, 1998, **10**, pp. 1171–1173

7 SRIVASTAVA, A.K., ZYSKIND, J.L., SUN, Y., ELLSON, J., NEWSOME, G., TKACH, R.W., CHRAPLYVY, A.R., SULHOFF, J.W., STRASSER, T.A., WOLF, C., and PEDRAZZANI, J.R.: 'Fast-link control protection of surviving channels in multiwavelength otical networks', *IEEE Photonics Technol. Lett.*, 1997, **9**, pp. 1667–1669

8 DAI, H., PAN, J.Y., and LIN, C.: 'All-optical gain control of in-line erbium-doped fiber amplifiers for hybrid analog/digital WDM systems', *IEEE Photonics Technol. Lett.*, 1997, **9**, pp. 737–739

9 RICHARDS, D.H., JACKEL, J.L., and ALI, M.A.: 'Multichannel EDFA chain control: A comparison of two all-optical approaches', *IEEE Photonics Technol. Lett.*, 1998, **10**, pp. 156–158

10 BERAN, J., SHERMAN, R., TAQQU, M.S., and WILINGER, W.: 'Long-range dependence in variable-bit-rate video traffic', *IEEE Trans. Commun.*, 1995, **43**, pp. 1566–1579

11 WILINGER, W., TAQQU, M.S., SHERMAN, R., and WILSON, D.V.: 'Self-similarity through high-variability: Statistical analysis of Ethernet LAN traffic at the source level', *IEEE/ACM Trans. Netw.*, 1997, **5**, pp. 71–86

12 CROVELLA, M.E., and BESTAVROS, A.: 'Self-similarity in World Wide Web traffic: Evidence and possible causes', *IEEE/ACM Trans. Netw.*, 1997, **5**, pp. 835–846

13 BONONI, A., TANCEVSKI, L., and RUSCH, L.A.: 'Large power swings in doped-fiber amplifiers with highly variable data', *IEEE Photonics Technol. Lett.*, 1998, **10**, pp. 131–133

14 TANCEVSKI, L., BONONI, A., and RUSCH, L.A.: 'Output power and SNR swings in cascades of EDFAs for circuit- and packet-switched optical networks', *J. Ligthwave Technol.*, 1999, **17**, pp. 733–742

15 BONONI, A., POTI, L., and AZZINI, A.: 'Measurement of power spread histograms in chains of EDFAs fed by multimedia burst-mode packet traffic'. Proc. European Conf. Opt. Commun., 1999, Nice, pp. II-104–105

16 SUN, Y., LUO, G., ZYSKIND, J.L., SALEH, A.A.M., SRIVASTAVA, A.K., and SULHOFF, J.W.: 'Model for gain dynamics in erbium-doped fibre amplifiers', *Electron. Lett.*, 1996, **32**, pp. 1490–1491

17 GEORGES, T., and DELEVAQUE, E.: 'Analytical modeling of high-gain erbium-doped fiber amplifiers', *Opt. Lett.*, 1992, **15**, pp. 1113–1115

18 ROCHETTE, M., GUY, M., LAROCHELLE, S., LAUZON, J., and TRÉPANIER, F.: 'Gain equalization of EDFAs with Bragg gratings', *IEEE Photonics Technol. Lett.*, 1999, **11**, pp. 536–538

19 ROSS, S.: 'A first course in probability' (Prentice Hall, 1998, 5th edn.)

20 TAQQU, M.S., TEVEROVSKY, V., and WILLINGER, W.: 'Estimators for long-range dependence: an empirical study', *Fractals*, 1995, **3**, pp. 785–788